Oscillatory Rise of Bubbles in Wormlike Micellar Fluids with Different Microstructures

Nestor Z. Handzy and Andrew Belmonte

W. G. Pritchard Laboratories, Department of Mathematics, Penn State University, University Park, Pennsylvania 16802, USA

(Received 10 January 2003; published 25 March 2004)

Previous observations of the nontransient oscillations of rising bubbles and falling spheres in wormlike micellar fluids were limited to a single surfactant system. We present an extensive survey of rising bubbles in another system, an aqueous solution of cetylpyridinium chloride and sodium salicylate, with and without NaCl, across a range of concentrations and temperatures. Two different types of oscillations are seen in different concentration ranges, each with its own temperature dependence. Rheological data identify these different hydrodynamic states with different fluid microstructures.

DOI: 10.1103/PhysRevLett.92.124501 PACS numbers: 47.55.Dz, 47.50.+d, 82.70.Uv

Fluids are often broadly categorized as either Newtonian or non-Newtonian, according to whether the Navier-Stokes equation does or does not accurately describe the fluid's motion. Newtonian fluids consist of molecules small enough to be approximated by point masses (such as air and water), while non-Newtonian consist of larger structures (such as polymers). This increased size affords greater degrees of freedom which leads to macroscopic viscoelasticity [1]. Fluids consisting of self-assembling cylindrical (or wormlike) micelles resemble polymeric fluids on the microscopic scale, with the added feature that their length distribution is determined by aggregation kinetics; micelles continually break and reform [2–4]. The molecular level physics is clearly more complicated for such fluids, and one can reasonably expect this will introduce a new set of flow properties to the class of non-Newtonian fluids.

Several novel results have been reported in both viscometric flows [5–9] and hydrodynamic flows [10–12] of various wormlike micellar fluids. Among these, a falling pendant drop at the bottom of a thin filament has been observed to slow to a complete stop before the filament suddenly ruptures [10]; this has been confirmed in other configurations [13]. Also, rising air bubbles and falling solid spheres have been observed to oscillate without reaching a terminal velocity [11,12]. While in polymer solutions a rising bubble displays a sharp nonaxisymmetric cusp, which remains unchanged during a steady rise [1,14], in wormlike micellar fluids the cusp periodically extends to a sharp point, then retracts to a blunt edge (see Fig. 1). It is likely that these new dynamics are a manifestation of the reversible scission reactions of the micelles, though the precise mechanism may be quite complicated. Another type of fluid is known to include scissionlike reactions at its microscale—associating polymer solutions—and falling sphere oscillations are reported in that system as well [15,16].

In this Letter, we report a detailed survey of the oscillatory motion of rising bubbles in a wormlike micellar fluid. To study the role of the aggregation kinetics of the micelles, both concentration and fluid temperature were varied over a wide range, unlike previous studies [11,12]. As these parameters change, different micellar architectures are possible—from short linear or branched micelles to crosslinked networks [17–19]. Four different dynamics were seen: Newtonian behavior at high temperatures, standard polymeric behavior, and two distinct oscillating responses occurring in different concentration ranges (Fig. 2). We performed steady rheology experiments to identify the fluid microstate, and found that transitions in the equilibrium structure match transitions in bubble dynamics. Critical temperature bounds were also found, which can be interpreted as a minimum length of micelle required for oscillations to occur, so that for certain concentrations the fluid may be tuned with temperature to make bubbles either oscillate, rise with a stable cusp, or rise as bubbles in a Newtonian fluid.

Nontransient oscillating bubbles were first observed in aqueous solutions of cetyltrimethylammonium bromide (CTAB) and sodium salicylate (NaSal) [11]; here we use another familiar system, cetylpyridinium chloride (CPCl) and NaSal, with the fixed ratio [NaSal]/[CPCl] = 1 (except for the NaCl experiments described below). Our choice for this ratio gives a solution of flexible cylindrical

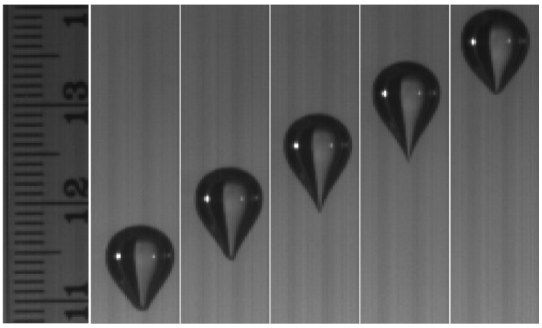

FIG. 1. Cusp shape change of an oscillating bubble rising through a 15 mM CPCl/NaSal (weight fraction $\varphi = 0.5\%$) solution at $T = 37.5\,^{\circ}\mathrm{C}$. The scale at left is marked in centimeters. Interval between pictures: 0.05 s.

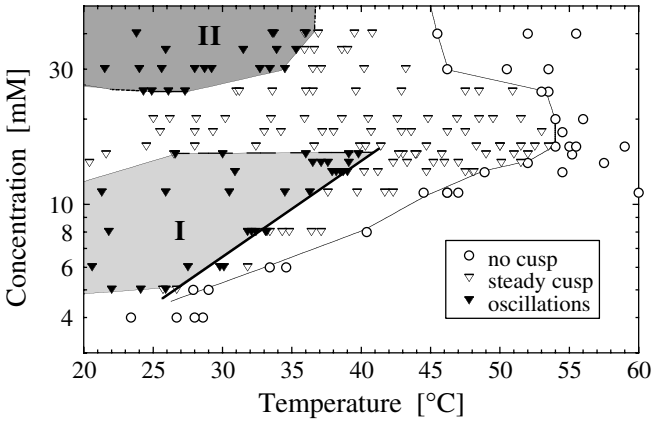

FIG. 2. Temperature and concentration phase diagram for the dynamics of rising bubbles in equimolar CPCl/NaSal, showing two distinct regions of oscillating behavior (shaded) labeled as I and II. The thick sloped line marking the temperature boundary for type I oscillations is an isoline of Eq. (1).

micelles analogous to polymer chains [5]. All experimental results are for a single rising bubble, with volumes ranging from 14 to 110 mm^3. The bubble is injected into the fluid at the bottom of a temperature controlled plastic cylinder (31 cm height, 5 cm diameter) using a syringe with a long stainless steel tube (inner diameter of either 1.0 or 1.5 mm). The ratio of the horizontal diameter of the bubble d to the cylinder diameter D is $d/D \leq 0.14$, and we have also checked that bubbles oscillate for $d/D \simeq 0.02$. Typical sizes of the Reynolds number (inertia) are $\mathrm{Re} \simeq 10^{-2}$–5, while the Deborah number (elasticity) ranged from $\mathrm{De} \simeq 1$–500, similar to values seen for oscillating bubbles and spheres in CTAB/NaSal [11,12]. Rheological data were taken with a Rheometrics RFS-III controlled rate of strain rheometer with circulating fluid temperature bath, using a stainless steel Couette geometry. Video images were made with a Kodak high speed charge coupled device camera.

We have studied concentrations from 4 to 40 mM (weight fractions $0.13\% \leq \varphi \leq 1.3\%$). From 5 to 15 mM, bubbles have a cusp which oscillates in length and changes shape (Fig. 1). While rising, the cusp lengthens (frames 1–4 in Fig. 1) during which the velocity as measured at the top of the bubble is nearly constant. At the apex of the extension, the tail abruptly retracts and the bubble jumps upward (frames 4–5). After this, it slows to a nearly constant velocity until the cycle repeats. Typically, bubbles begin to oscillate within 10 s of their formation, with a similar time between jumps. These clearly visible oscillations, which we call type I, are apparently not a transient effect; we have observed their persistence for rise distances over 1 m, during which there were more than 30 oscillations in ~35 s (for 8 mM CPCl/NaSal), and velocities more than doubled during a jump. This is the typical type I behavior in the temperature ranges shown in Fig. 2, consistent with the oscillations observed in CTAB/NaSal [11].

Above a critical temperature in the type I range (Fig. 2), bubbles have a sharp cusp which does not change in length ("steady cusp" in Fig. 2) and velocities smoothly reach a steady state; the oscillatory instability vanishes. By 60 °C, the solutions appear Newtonian ("no cusp" in Fig. 2): large enough bubbles are ellipsoidal and undergo the well-known side-to-side oscillations [20]. In this temperature range, the micelles must be predominantly spherical or short rigid rods [21].

Upon increasing the concentration from 15 to 16 mM ($\varphi = 0.5\%$ to 0.53%), *all oscillations cease.* Bubbles rise steadily with a stable cusp for concentrations up to 20 mM; there are no temperatures at which oscillations occur (Fig. 2). It is striking that a rising bubble would be so affected by so slight a concentration change. Note the transition temperature from polymeric to Newtonian behavior reaches a maximum at this concentration (Fig. 2).

More surprising is the reemergence of oscillations for concentrations from 25 to 40 mM. Yet these the oscillations, which we call type II, are visibly different from type I oscillations; the shape change involves the entire bubble, whereas in type I it seems restricted to the tail. A type II oscillation begins with a constriction in width near the top, while the whole bubble lengthens. This constriction then travels downward, as if the bubble were squeezing through a hoop. Defining $w_{\max}$ to be the maximum (relaxed) width (at its waist), $w_{\min}$ the most constricted width, and $\Delta w = w_{\max} - w_{\min}$, we found $\Delta w/w_{\max} = 0.13$ in type II fluids and 0.04 in type I. Length extensions, however, were $\Delta l/l_{\min} = 0.25$ in type II and 0.27 in type I; for bubbles in CTAB/NaSal, $\Delta l/l_{\min} = 0.26$ [11]. This previous study revealed only one type of oscillation, which from the shape dynamics we identify as type I [11].

Although wormlike micelles consist of surfactants, it is unlikely that surface tension plays a role in the bubble oscillations, since falling rigid spheres also oscillate [12]. Thus, our observation of two oscillation types suggests the viscoelasticity of the fluid changes with concentration. We address this through rheology, controlling the shear strain rate $\dot{\gamma}$ and recording the effective viscosity, $\eta_{\mathrm{eff}} = \sigma_{xy}/\dot{\gamma}$, where σ_{xy} is the steady shear stress. Transient tests were also performed to ensure that steady state was achieved. Figure 3(a) shows η_{eff} vs $\dot{\gamma}$ for fluids in the oscillating and nonoscillating concentration ranges at 30 °C. Most fluids shear thin—η_{eff} decreases with $\dot{\gamma}$—however, fluids below 5 mM shear thicken (η_{eff} increases above the zero shear viscosity η_0, defined as the plateau value at low $\dot{\gamma}$), typically requiring ~100 s to reach steady state [9]. Bubbles tested in fluids below 5 mM showed no oscillations. While there is a noticeable difference in the rheology upon increasing from 20 to 30 mM, 30 and 40 mM (type II region) are strikingly similar; they maintain η_0 over a broad $\dot{\gamma}$ range. More interestingly, η_0 decreases with concentration.

Pursuing the dependence of η_0 on φ further indicates transitions in fluid microstructure [Fig. 3(b)]. The

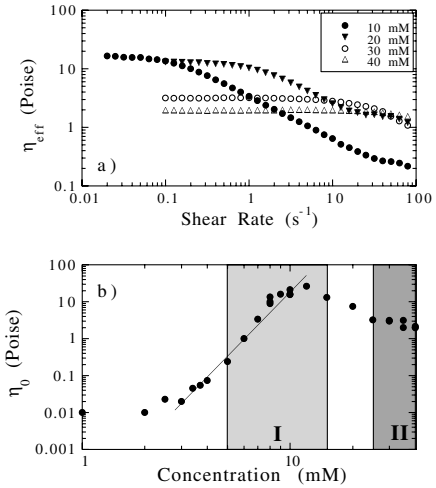

FIG. 3. Rheology of equimolar CPCl/NaSal at 30 °C: (a) η_{eff} vs $\dot{\gamma}$ for 10, 20, 30, and 40 mM; (b) η_0 as a function of concentration. The shaded regions mark the concentration ranges of bubble oscillations, and the sloped line corresponds to $\eta_0 \sim \varphi^{5.8}$.

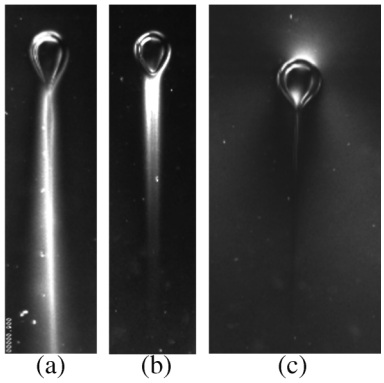

FIG. 4. Birefringent images of the wake behind a bubble rising in CPCl/NaSal at $T = 24$ °C: (a) 10 mM; (b) 20 mM; (c) 35 mM. Each image is 6.5 cm high. Reynolds and Deborah numbers for each image are (a) Re $\simeq$ 4.72, De $\simeq$ 250; (b) Re $\simeq$ 0.02, De $\simeq$ 6; (c) Re $\simeq$ 1.1, De $\simeq$ 1.8.

transition at low concentration to rapid η_0 growth marks the overlap concentration $\varphi^* \simeq 3$ mM, below which is the dilute regime. Above φ^* is the semidilute state, in which micelles exist as individual entangled worms [22]. Here $\eta_0 \sim \varphi^{5.8}$, close to the value 5.4 associated with stress relaxation by reptation [18,23]. The semidilute regime ends near $\varphi \simeq 12$–15 mM, followed by an extraordinary decrease of η_0 with concentration, continuing to $\varphi \simeq 30$ mM, after which η_0 varies weakly.

The dramatic change in the concentration dependence of η_0 indicates a transition in the equilibrium fluid structure, which coincides with the loss of type I oscillations. It may be that entangled micelles in the semidilute range have begun to fuse at entanglement points, forming a crosslinked network [18,23–25]. The junction nodes are free to slide along the micelles in such a formation, which would account for the decrease in viscosity [18]. If the ratio of crosslinks to entanglement points grows as η_0 decreases, then the new state would be fully formed where η_0 stabilizes near $\sim$30 mM (1%), the start of type II oscillations. Note that a crosslinked network state has also been proposed for CTAB/NaSal at $\varphi \simeq 1\%$ [26].

Such transitions in micellar morphology would naturally lead to transitions in mechanisms for stress relaxation, which should be observable in the stress field around the rising bubble. These transitions are made evident with birefringent visualization, shown in Fig. 4 for the three concentration regimes. Optical birefringence is a well-known technique for visualizing stress in non-Newtonian fluids [27], especially effective for wormlike micellar fluids [28]. Figure 4(a) (10 mM) shows the localization of stress in the wake of a type I oscillating bubble. This birefringent tail mirrors the dynamics of the bubble's cusp (Fig. 1), and when it retracts the birefringent tail suddenly disperses to the sides. The flow in the bubble wake is nearly in uniaxial extension [29], and the birefringent tail suggests a strong relation to a filament whose rupture [10] may be related to the oscillations. At 20 mM a shorter tail is seen [Fig. 4(b)], whose length remains constant (similar to the bubble tail). Figure 4(c) corresponds to type II oscillations (35 mM), in which three equally spaced birefringent bands indicate a broader distribution of stress. This pattern is essentially unaltered during an oscillation. Note that De decreases from type I to type II, with an intermediate value for nonoscillating bubbles (Fig. 4 caption), contradicting the implicit critical De condition for oscillations in [12].

It is natural to ask how these differences correlate to the rheology. We estimate the shear rates near the surface using the Stokes flow solution around a spherical bubble [1] for the data in Fig. 4. The values are 5.8 s^{-1} (10 mM), 0.5 s^{-1} (20 mM), and 3.4 s^{-1} (35 mM). This places type I oscillations firmly in the shear thinning region of Fig. 3(a), while type II is in the η_0 plateau. The nonoscillating bubble shear rate lies in the η_0 plateau but near the rate where thinning begins. While this supports the notion that different mechanisms are responsible for different oscillations, it provides no clear indication of the oscillation mechanism.

The length distribution of the individual worms in the type I region (semidilute) should depend on temperature and concentration. In equilibrium, the average length of a wormlike micelle L_0 can be described with the mean field approximation [2,3,21]:

$$L_0(\phi, T) \sim \sqrt{\phi} e^{E/2kT}, \tag{1}$$

where ϕ is the total amphiphile concentration, k is Boltzmann's constant, T is temperature, and E is the scission energy required to break one micelle into two. Estimates based on light scattering measurements for E are on the order of 10 kT [2,17,30]—much lower than the covalent bonds of polymers, yet large enough for some

micelles to reach appreciable lengths against thermal fluctuations [2]. The flow near the bubble may increase the equilibrium length, and there is evidence that shear-induced structures (SIS) much larger than individual micelles form in such flow [9,31–34]. We assume simply that, for the type I region, L_0 is the relevant quantity determining if the bubble will oscillate. Specifically, we attribute the oscillations to a breaking instability of the elongated micelles or SIS in the wake, occurring only if L_0 exceeds some critical value. Using Eq. (1), the solid line in Fig. 2 corresponds to a scission energy of $E = 1.01 \times 10^{-19}$ J, about 24 kT.

Type II oscillations may have a much simpler dependence on temperature; the three data points in Fig. 2 (30, 35, and 40 mM) are within 1 °C of each other over a 10 mM range, the same span as the type I region. This suggests the condition $T \lesssim T_c = 36\,^{\circ}\mathrm{C}$ for the onset of type II oscillations, possibly representing a constant energy difference between an entangled state ($T > T_c$) and a crosslinked network of micelles. Testing this would require further experimentation at higher concentrations.

The two different oscillations we have observed appear linked to two different microstructures. We extended our study to include the well characterized ternary system CPCl-NaSal diluted in NaCl, with [NaSal]/[CPCl] = 0.5 [8,22,35]. We tested several concentrations [36] for jumping bubbles in our apparatus, at $T = 30\,^{\circ}\mathrm{C}$, a temperature central to both type I and II oscillations (Fig. 2). We observed no oscillations or any behavior different from steadily rising bubbles in conventional polymeric fluids [14]. This ternary system is known to consist of entangled wormlike micelles, in which $\eta_0 \sim \varphi^{3.3}$, indicating that micellar breaking occurs on a shorter time scale than reptation [2,22]; in contrast for our fluids $\eta_0 \sim \varphi^{5.8}$. Evidently, the oscillatory motion of rising bubbles is not characteristic of this "fast-breaking" limit [2,37], and we conclude that type I oscillations are in the "slow-breaking" limit.

Our study of rising bubbles in various wormlike micellar fluids indicates that, while scission reactions may be necessary for oscillations, there are other conditions. The discovery of a second type of oscillation provides another example of how microscale dynamics and architecture couple to produce macroscopic instabilities. It now seems that wormlike micellar fluids are the most generic complex fluids as far as rising bubbles are concerned, since all known material-dependent dynamics can occur at different temperatures or concentrations. More surprisingly, the rise of an air bubble has been shown to be extraordinarily sensitive to fluid microstructure.

We thank A. Jayaraman, J. Jacobsen, P. Olmsted, T. Podgorski, and L. Walker for valuable discussions, and R. Geist, D. Henderson, and M. Sostarecz for experimental assistance. A. B. acknowledges support from the Sloan Foundation and the National Science Foundation (CAREER Grant No. DMR-0094167).

[1] R. Bird, R. Armstrong, and O. Hassager, *Dynamics of Polymeric Liquids*, (Wiley, New York, 1987), 2nd ed.
[2] M. Cates and S. Candau, J. Phys. Condens. Matter **2**, 6869 (1990).
[3] J. Israelachvili, *Intermolecular and Surface Forces* (Academic, New York, 1991), 2nd ed.
[4] *Micelles, Membranes, Microemulsions, and Monolayers*, edited by W. Gelbart *et al.* (Springer, New York, 1994).
[5] H. Rehage and H. Hoffmann, J. Phys. Chem. **92**, 4712 (1988).
[6] T. Shikata and H. Hirata, J. Non-Newtonian Fluid Mech. **28**, 171 (1988).
[7] C. Grand, J. Arrault, and M. Cates, J. Phys. II **7**, 1071 (1997).
[8] S. Lerouge, J.-P. Decruppe, and J.-F. Berret, Langmuir **16**, 6464 (2000).
[9] C. Liu and D. Pine, Phys. Rev. Lett. **77**, 2121 (1996).
[10] L. Smolka and A. Belmonte, J. Non-Newtonian Fluid Mech. **115**, 1 (2003).
[11] A. Belmonte, Rheol. Acta **39**, 554 (2000).
[12] A. Jayaraman and A. Belmonte, Phys. Rev. E **67**, 65301 (2003).
[13] J. Rothstein, J. Rheol. **47**, 1227 (2003).
[14] Y. Liu, T. Liao, and D. Joseph, J. Fluid Mech. **304**, 321 (1995).
[15] A. Mollinger, E. Cornelissen, and B. van den Brule, J. Non-Newtonian Fluid Mech. **86**, 389 (1999).
[16] P. Weidman, B. Roberts, and S. Eisen, *Progress in Nonlinear Science, Proceedings III*, edited by V. D. Shalf-eev (Nizhny Novgorod Press, Nizhny Novgorod, 2002), p. 103.
[17] M. In, G. Warr, and R. Zana, Phys. Rev. Lett. **83**, 2278 (1999).
[18] J. Appell *et al.*, J. Phys. II **2**, 1045 (1992).
[19] V. Schmitt, F. Lequeux, A. Pousse, and D. Roux, Langmuir **10**, 955 (1994).
[20] R. Hartunian and W. Sears, J. Fluid Mech. **3**, 27 (1957).
[21] Ben-Shaul and Gelbart (Ref. [4]).
[22] J.-F. Berret, J. Appell, and G. Porte, Langmuir **9**, 2851 (1993).
[23] S. Candau *et al.*, J. Phys. IV **3**, 197 (1993).
[24] T. Drye and M. Cates, J. Chem. Phys. **96**, 1367 (1992).
[25] P. Pincus, Science **290**, 1307 (2000).
[26] F. Lequeux and S. Candau, in *Theoretical Challenges in the Dynamics of Complex Fluids*, edited by T. McLeish (Kluwer, Dordrecht, 1997).
[27] G. Fuller, Annu. Rev. Fluid Mech. **22**, 387 (1990).
[28] Y. Hu, S. Wang, and A. Jamieson, J. Rheol. **37**, 531 (1993).
[29] O. Harlen, J. Rallison, and M. Chilcott, J. Non-Newtonian Fluid Mech. **34**, 319 (1990).
[30] S. Kwon and M. Kim, Phys. Rev. Lett. **89**, 258302 (2002).
[31] P. Boltenhagen *et al.*, Europhys. Lett. **38**, 389 (1999).
[32] S. Keller *et al.*, Phys. Rev. Lett. **80**, 2725 (1998).
[33] E. Wheeler, P. Fischer, and G. Fuller, J. Non-Newtonian Fluid Mech. **75**, 193 (1998).
[34] P. Fischer, Rheol. Acta **39**, 234 (2000).
[35] J.-F. Berret, D. C. Roux, and G. Porte, J. Phys. II **4**, 1261 (1994).
[36] We tested [CPCl] = 30, 40, 50, 60, 70, and 80 mM, with [NaSal]/[CPCl] = 0.5 and 500 mM NaCl.
[37] J.-F. Berret, Langmuir **13**, 2227 (1997).